Optics Letters

On-chip wavelength locking for photonic switches

Akhilesh S. P. Khope,* Takako Hirokawa, Andrew M. Netherton, Mitra Saeidi, Yujie Xia, Nicolas Volet, Clint Schow, Roger Helkey, Luke Theogarajan, Adel A. M. Saleh, John E. Bowers, and Rod C. Alferness

Electrical and Computer Engineering Department, University of California, Santa Barbara (UCSB), California 93106, USA
**Corresponding author: akhileshsk@ece.ucsb.edu*

Received 6 September 2017; revised 27 October 2017; accepted 30 October 2017; posted 30 October 2017 (Doc. ID 305974); published 27 November 2017

We present an on-chip wavelength reference with a partial drop ring resonator and germanium photodetector. This approach can be used in ring-resonator-based wavelength-selective switches where absolute wavelength alignment is required. We use the temperature dependence of heater resistance as a temperature sensor. Additionally, we discuss locking speed, statistical variation of heater resistances, and tuning speed of the switches.

OCIS codes: (200.6715) Switching; (250.5300) Photonic integrated circuits; (130.4815) Optical switching devices.

https://doi.org/10.1364/OL.42.004934

Wavelength-selective switches promise greater capacity and flexibility in data centers when used with electronic packet switches [1]. Multiple variants of fat pipe switches have been demonstrated in silicon photonics in [2–4]. Ring-resonator-based wavelength-selective switches have been demonstrated by different groups [5,6], and provide the advantage of fine granularity wavelength switches which better fit the traffic patterns in datacenters.

We proposed a flexible ring-resonator-based architecture in [7], where any set of multiple wavelengths could be switched between input-output pairs. In [7] we also established that two rings per cross point are sufficient for a ring-based crossbar switch where the number of wavelengths per port are equal to the number of ports. Such micro-ring-based switches that can establish a connection with any one or a set of multiple wavelengths from a WDM signal require a robust wavelength locking scheme. The locking scheme in this problem is different from other approaches [8–12], where a ring resonator or a bank of resonators can lock to a particular or all wavelengths in a WDM signal, but one cannot be certain to which wavelength a particular ring is locked without an external optical spectrum analyzer (OSA). For this we need an absolute wavelength reference on chip to lock any switch node to a given wavelength of choice. In this Letter we demonstrate such an approach, which requires only an approximate tuning curve of the ring resonators, does not require an external monitor signal for wavelength identification, and can lock rings at different stage temperatures. Preliminary results from this configuration were presented in [13]. In this Letter we present locking time, statistical variation of ring resonators, and detailed discussions regarding the performance of the switch.

Figure 1(a) shows a schematic of the experimental setup of the wavelength locking experiment. A tunable laser (Yenista Tunics T100S-HP) is used to inject a wavelength at 1557 nm with TE polarization into the device. We control the polarization of light with a Newport polarization controller (PC: Model F-POL-APC). The chip is mounted on top of a thermo-electric Cooler (TEC), which we use to change the stage temperature with the help of a thermister and ILX temperature controller (Model LDT-5980). Figure 1(b) shows the experimental setup with the TEC, thermister, electrical probes, and input and outputs of the device under test (DUT).

Figure 1(c) shows the schematic of the architecture of the switch. Each switch matrix unit cell has L second-order ring resonators that can select up to L wavelengths from incoming WDM channels and a waveguide crossing. The free spectral range (FSR) of the ring resonators should be designed to fit all the channels, and the rings have to be tuned by thermal tuning as tuning across all channels is required. For example, for 8 WDM channels at 200 GHz channel spacing, an FSR of at least 1.6 THz (12.8 nm) is required. In our experiment, we used an FSR of 26 nm. The synchronous time slotted operation of the switch with centralized arbiter implies an input queued switch architecture [7]. The DUT is shown by the dashed box in Fig. 1(c) and by the micrograph of Fig. 1(d). Our locking experiment was conducted by tuning only one of the two second-order ring resonators. The optical output is recorded by an OSA (Yokogawa AQ6370).

These devices were a part of the initial release of the AIM Photonics Process Design Kit (PDK). The switch ring resonators were equipped with thermo-optic and electro-optic tuners. In our experiments we used thermal tuning due to a higher tuning efficiency of 0.84 nm/mW and negligible loss penalty as compared to electro-optic tuning. For electro-optic tuning, the resonance wavelength was blueshifted and attenuated with a loss of 3.6 dB/nm. The 3 dB bandwidth of the resonators was 40 GHz and with better than 30 dB of out of band rejection at the drop port. The measured insertion loss of each second-order

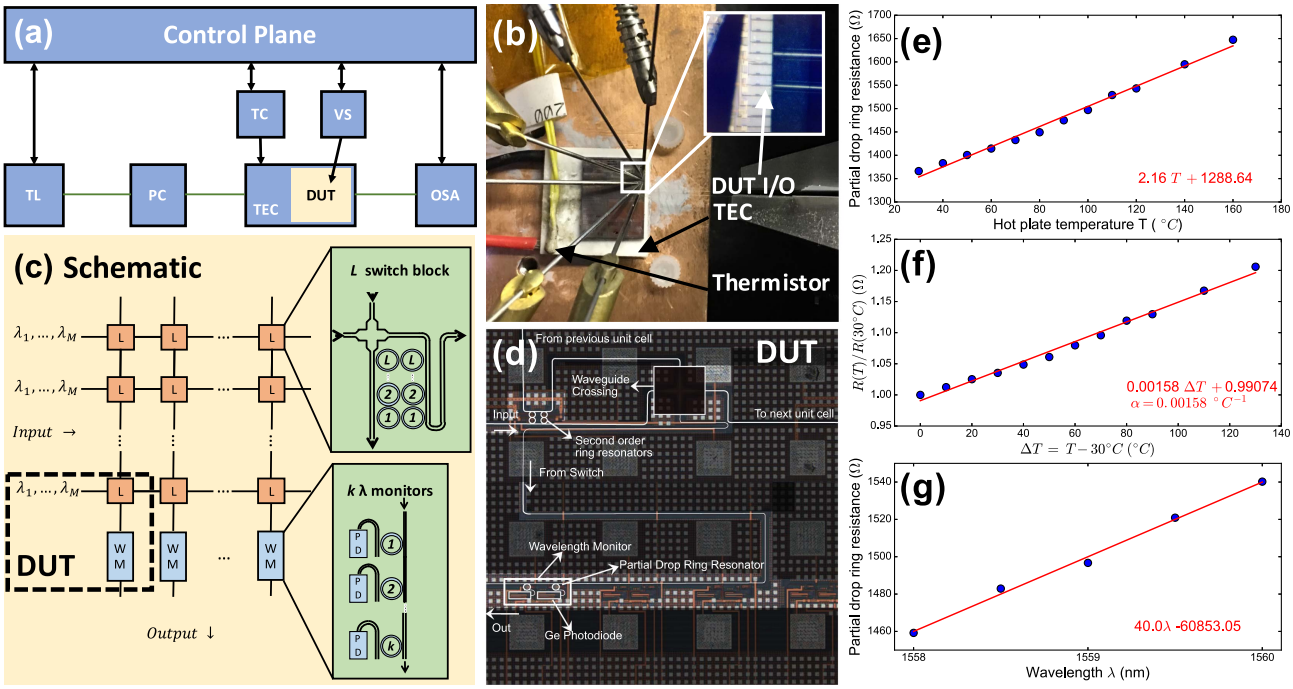

Fig. 1. (a) Schematic of the setup. **TL**, tunable laser; **PC**, polarization controller; **DUT**, device under test; **TEC**, thermo-electric Cooler; **TC**, temperature controller; **OSA**, optical spectrum analyzer; **VS**, voltage source. (b) Test setup of the experiment. (c) General schematic of wavelength-selective switch shown has L second-order ring switches and a waveguide crossing at each intersection and k wavelength monitors (**WM**) at the bottom of each column, which have an on-chip photodiode (**PD**). The DUT is marked with a dashed box. (d) Micrograph of the switch. (e) Partial drop ring heater resistance versus hot plate temperature. (f) Verification of Eq. (1). (g) Tuning map, partial drop ring heater resistance versus locked wavelength at 20°C.

ring was measured at 1.2 dB for wavelengths off resonance at the through port and 3.5 dB on resonance at the drop port. Cleaved single-mode fibers are used for optical coupling. The light is edge-coupled into the chip with a Si_3N_4/Si mode converter with a typical coupling loss of 3 dB in the C band.

The wavelength monitor (WM) consists of a thermally tunable partial drop ring resonator that is designed to drop 10% of the output power at a germanium (Ge) photodiode. These resonators were provided by the foundry PDK and their design was similar to [14]. If these partial drop resonators are tuned to the correct wavelength, the second-order switch can be tuned to maximize the photodiode current captured by the Ge photodiode. However, a change in the ambient temperature changes the resonant wavelength of the WM. This problem can be circumvented by using the resistance of the heater in the partial drop filter as a temperature sensor. The resistance of the partial drop resonator heater is measured as a function of hot plate temperature T from 30°C to 140°C at a bias voltage of 0.1 V, as given in Fig. 1(e), and the linear relation given by Eq. (1) is verified with a linear polynomial fit in Fig. 1(f):

$$R(T) = R(30°\text{C})(1 + \alpha(T - 30°\text{C})), \quad \textbf{(1)}$$

where T is the resistor temperature in °C and α is the temperature coefficient of resistance of $1.58 \cdot 10^{-3}$°C^{-1} from Fig. 1(f). This fit demonstrates that resistance can be used as a temperature sensor. At a stage temperature of 20°C, voltages on second-order ring heaters (V_1, V_2) are optimized with the OSA, then we choose the voltage on the partial drop resonator (V_{WM}) corresponding to the highest photodetector current. The value of resistance at this V_{WM} versus the optimized wavelength λ gives the tuning map of $R(\lambda)$ measured at stage temperature of 20°C given in Fig. 1(g). In Algorithm 1, we describe the locking procedure. Here a prior on the number of incoming WDM channels is assumed known and step 4 is useful for locking in the presence of multiple channels.

Algorithm 1. On-Chip Locking Algorithm

1: **procedure** Lock (V_1, V_2) ▷ for a given λ, $R(\lambda)$
2: At $T = T_{stage}$ and λ set V_{WM} corresponding to $R(\lambda)$
3: Coarse sweep in (V_1, V_2) with $V_1 = V_2$, and record PD current (I_{PD})
4: Pick a guess voltage $V_{guess} = V_1 = V_2$ corresponding to peak in I_{PD} corresponding to channel number
5: optimize (V_1, V_2) to maximize I_{PD}.

Next we present our results on locking in the presence of a single channel and two channels spaced at $\Delta\nu =$ 100, 200 GHz. Figure 2(a) shows the temperature dependence of the resonant wavelength. The resonant wavelength of the ring changes by 80 pm/K. In this figure, the voltages on the switch heaters were optimized for highest power transmission at 40°C and then the stage temperature was changed to 20°C and 30°C with the heaters set to voltages corresponding to 40°C. We then use our wavelength locking scheme to change the switch heater voltages with the help of the WM and lock wavelengths within 20 pm of the target wavelength. The tunable laser used for measurement had a 20 pm accuracy. The results can be seen in Fig. 2(b).The transfer function of the

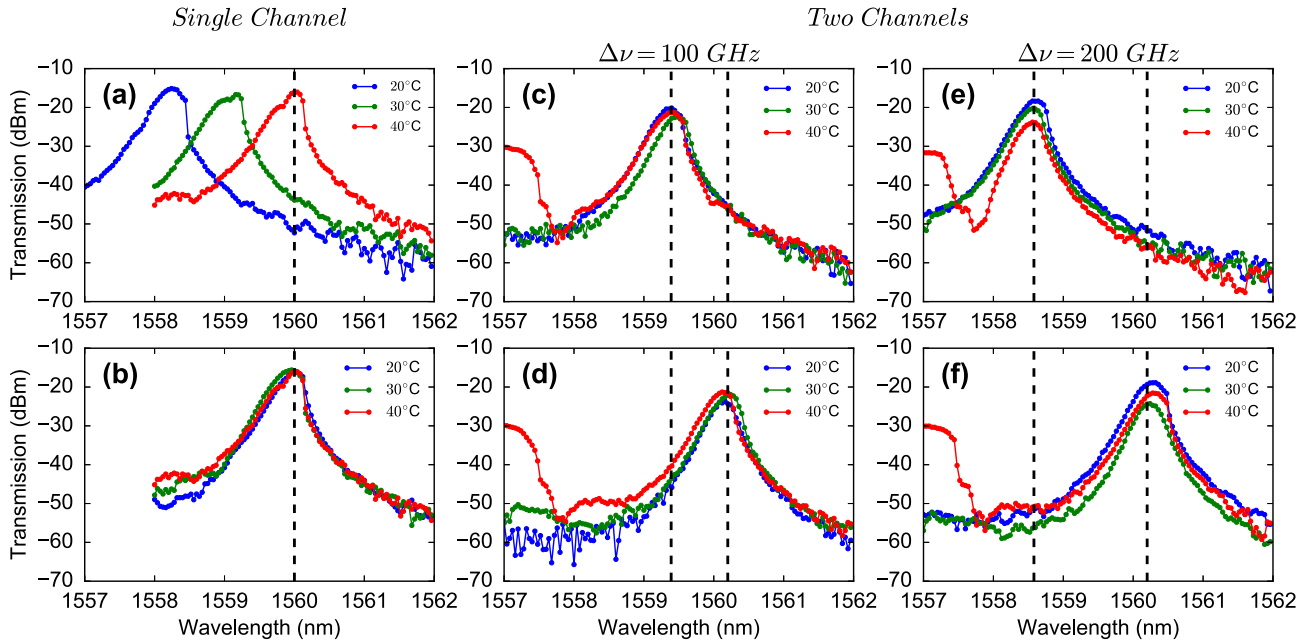

Fig. 2. Transfer function of the second-order resonator after locking to predefined wavelengths at different stage temperatures. Wavelengths to which the ring is locked is given as a black dashed line. (a) and (b) show results before and after locking in the presence of input single wavelength. (c) and (d) show results after locking to two channels separated by $\Delta\nu = 100$ GHz. (e) and (f) show results for $\Delta\nu = 200$ GHz.

drop port spectra of the second-order ring is recorded here after the locking.

Figures 2(c) and 2(d) show before and after locking results in the presence of two channels spaced at $\Delta\nu = 100$ GHz. Figures 2(e) and 2(f) show before and after locking in the presence of two channels spaced at $\Delta\nu = 200$ GHz. In these experiments system loss was measured at 20 dB and input power on both wavelengths was 10 dBm. In the transfer function corresponding to 40°C in Figs. 2(c), 2(d), 2(e), and 2(f) the peak corresponding to the other second-order switch in the unit cell with unoptimized heater voltages is also visible. The optimization is run with stochastic hill climbing (SHC) [15] with a noise standard deviation of 50 mV to limit search space around V_{guess}.

Figure 3(a) shows the speed of different algorithms used to optimize the heater voltages applied to the second-order switch ring. We compare three different optimization methods, namely the Nelder–Mead [16], the SHC, and Powell's algorithms [17]. SHC, specifically in this case random mutation hill climbing, is a type of genetic algorithm where we apply stochastic noise to the voltages and update the best guess to the heater voltages depending on the fitness criteria (transmission). Because of the stochastic nature of the search, the locking time is not deterministic and this is shown by the multiple blue

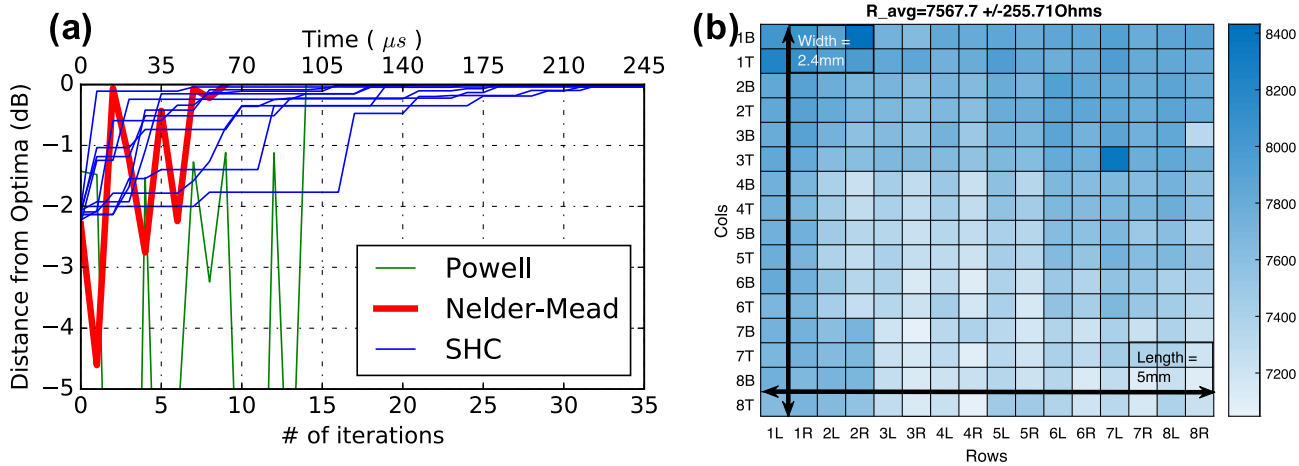

Fig. 3. (a) Locking speed of different algorithms, with Nelder–Mead being the fastest locking algorithm. Here, the distance from optima is the separation from the terminal optimized transmission of the second-order ring resonator. (b) Measured variation of the second-order ring heater resistance across the switch chip at a stage temperature of 20°C, with an average value of 7568Ω, and a standard deviation of 256Ω.

trajectories in the figure. Both Nelder–Mead and Powell are derivative-free algorithms which give deterministic trajectories and locking times. These were implemented with the minimization module of SciPy library of Python. The top axis of locking time is generated assuming each iteration takes 7 μs, which is the measured thermal time constant. The heuristic algorithms do not terminate on a non-optimal local maxima as the second-order switch transmission is a unimodal function of heater voltages, i.e., there exists only one maximum. These heuristic algorithms are also accurate and faster than a grid search over the two heater voltages of the second-order resonators since the function is unimodal.

The main reason why we pursued this approach was that there was an 8% standard deviation in heater resistance across the switch chip, as shown in Fig. 3(b). A total of 256 heater resistances from 128 second-order rings were used to measure this standard deviation. The size of the switch die across which measurements are done is 5 mm × 2.4 mm. This means that one cannot generate a tuning curve for a single resonator and use that to lock other ring resonators as each resonator will have a different tuning curve.

In Fig. 2, we were limited by the temperature range for which our approach of absolute wavelength locking worked from 20°C–40°C. This was due to the limited tuning of the ring resonators fabricated. Though the resonators were designed to be fully tunable across an FSR of 26 nm, we saw performance degradation of the heater after tuning by ∼8 nm. Further investigation of the tuning limits of these structures is needed, but tuning across this fraction of the FSR still allows for useful switching operation.

An advantage of this method is the ability to be resistant to thermal cross talk across the switch. The wavelength monitors can be placed away from the switch rings and multiple ring resonators can be optimized simultaneously with two or more wavelength monitors in a column. For example, if two ring resonators are placed close to each other, their voltages can be optimized simultaneously with the WM as reference. These voltages will self-adjust according to the thermal cross-talk penalty to maximize drop power at a particular wavelength.

Fortunately, it was not necessary to compensate for thermal cross talk, as the observed thermal cross talk was small. In most cases, the layout of the switch is pad limited and if the pads are laid out in a flip-chip configuration, for example in a square grid at 150 μm pitch, the switch rings can be placed far apart to avoid significant thermal cross talk. This is because the footprint of a ring resonator is 20 μm × 10 μm, which is small compared to 150 μm pitch. To scale such switches, optical interposers might be used in the future and the rings can be placed closer together for tighter packing and this can increase the thermal cross talk. The motivation behind placing k WM per column in Fig. 1(c) is that speed of locking can be parallelized. We placed identical partial drop rings in our layout. If the number of channels is equal to the number of WMs then partial drop rings with different resonant wavelengths can be used.

To conclude, we present an approach to bias and stabilize ring-resonator-based wavelength-selective switches where absolute wavelength alignment is required. We use the temperature dependence of heater resistance as a temperature sensor to stabilize the ring switching wavelengths.

Funding. American Institute of Manufacturing Photonics.

Acknowledgment. The authors thank AIM Photonics for the foundry services (https://aim.ucsb.edu/ and http://www.aimphotonics.com/). The authors also thank Alfredo Torres for wirebonding, and Tin Komljenovic, Eric Stanton, Alexander Spott, and Tony Huang at UCSB; Ben Moss and Erman Timurdogan at Analog Photonics; and Jeremiah Hebding and Brett Attaway at SunyPoly for insightful discussions.

REFERENCES

1. A. A. M. Saleh, A. S. P. Khope, J. E. Bowers, and R. C. Alferness, *OptoElectronics and Communications Conference (OECC) and Photonics in Switching (PS)* (2016).
2. K. Tanizawa, K. Suzuki, M. Toyama, M. Ohtsuka, N. Yokoyama, K. Matsumaro, M. Seki, K. Koshino, T. Sugaya, S. Suda, G. Cong, T. Kimura, K. Ikeda, S. Namiki, and K. Hitoshi, Opt. Express **23**, 17599 (2015).
3. N. Dupuis, A. V. Rylyakov, C. L. Schow, D. M. Kuchta, C. W. Baks, J. S. Orcutt, D. M. Gill, W. M. Green, and B. G. Lee, J. Lightwave Technol. **35**, 615 (2017).
4. P. DasMahapatra, R. Stabile, A. Rohit, and K. A. Williams, IEEE J. Sel. Top. Quantum Electron. **20**, 1 (2014).
5. A. W. Poon, X. Luo, F. Xu, and H. Chen, Proc. IEEE **97**, 1216 (2009).
6. D. Nikolova, D. M. Calhoun, Y. Liu, S. Rumley, A. Novack, T. Baehr-Jones, M. Hochberg, and K. Bergman, Microsyst. Nanoeng. **3**, 16071 (2017).
7. A. S. Khope, A. A. Saleh, J. E. Bowers, and R. C. Alferness, *IEEE Optical Interconnects (OI) Conference* (2016), pp. 48–49.
8. K. Padmaraju, D. F. Logan, T. Shiraishi, J. J. Ackert, A. P. Knights, and K. Bergman, J. Lightwave Technol. **32**, 505 (2014).
9. S. Grillanda, M. Carminati, F. Morichetti, P. Ciccarella, A. Annoni, G. Ferrari, M. Strain, M. Sorel, M. Sampietro, and A. Melloni, Optica **1**, 129 (2014).
10. Y. Li and A. W. Poon, *Conference on Lasers and Electro-Optics (CLEO)* (2015), pp. 1–2.
11. A. Gazman, C. Browning, Z. Zhu, L. P. Barry, and K. Bergman, "Automated thermal stabilization of cascaded silicon photonic ring resonators for reconfigurable WDM applications" (2017), https://www.semanticscholar.org/paper/Automated-Thermal-Stabilization-of-Cascaded-Silico-Gazman-Browning/3b6814b12293358679a186e184d6df9ad4a641db?tab=abstract.
12. P. Dong, R. Gatdula, K. Kim, J. H. Sinsky, A. Melikyan, Y.-K. Chen, G. de Valicourt, and J. Lee, Opt. Express **25**, 16040 (2017).
13. A. Khope, A. M. Netherton, T. Hirokawa, N. Volet, E. Stanton, C. Schow, R. Helkey, A. Saleh, J. Bowers, and R. C. Alferness, Photonics in Switching (2017), pp. PTh1D-3.
14. Z. Su, E. Timurdogan, J. Sun, M. Moresco, G. Leake, D. Coolbaugh, and M. R. Watts, *Conference on Lasers and Electro-Optics (CLEO)* (2014), pp. 1–2.
15. M. Mitchell, J. Holland, S. Forrest, and D. Whitley, Foundations of Genetic Algorithms **2**, 109 (2014).
16. J. A. Nelder and R. Mead, Comput. J. **7**, 308 (1965).
17. M. J. Powell, Comput. J. **7**, 155 (1964).